arXiv:1703.10479v3 [gr-qc] 27 Apr 2017

Accretion onto a noncommutative geometry inspired black hole

Rahul Kumar[1,*] and Sushant G. Ghosh[1,2,3,†]

[1] *Centre for Theoretical Physics, Jamia Millia Islamia, New Delhi 110025 India*
[2] *Multidisciplinary Centre for Advanced Research and Studies (MCARS), Jamia Millia Islamia, New Delhi 110025, India*
[3] *Astrophysics and Cosmology Research Unit, School of Mathematics, Statistics and Computer Science, University of KwaZulu-Natal, Private Bag X54001, Durban 4000, South Africa*

The spherically symmetric accretion onto a noncommutative (NC) inspired Schwarzschild black hole is treated for a polytropic fluid. The critical accretion rate $\dot{M}$, sonic speed a_s and other flow parameters are generalised for the NC inspired black hole and compared with the results obtained for the standard Schwarzschild black holes. We also derive explicit expressions for gas compression ratios and temperature profiles below the accretion radius and at the event horizon. This analysis is a generalisation of Michel's solution to the NC geometry. Owing to the NC corrected black hole, the accretion flow parameters have also been modified. It turns out that $\dot{M} \approx M^2$ is still achievable but r_s seems to be substantially decreased due to NC effects, that in turn does affect the accretion process.

I. INTRODUCTION

The process by which compact massive astronomical objects capture the ambient matter present in the interstellar medium, and leads to increase in their mass (and possibly their angular momentum also) is called *accretion* [1]. It is one of the most ubiquitous processes in the Astrophysics. This accretion of gas by compact objects is likely to be the source of energy of observed X-rays binary, quasar and active galactic nuclei. During accretion, kinetic energy of in-falling gas increase on the essence of gravitational energy and subsequently result in the increase in radiant energy of the object. The history of research on the accretion of an ideal fluid onto a compact object begins with the work of Hoyle and Lyttleton [2], who studied the effects of accretion onto the change in terrestrial climate and subsequently, the considerable change in the radiation emitted. In their work, they neglect the pressure effects. Later in this extension, Bondi [3] in his pioneering work studied the stationary, spherically symmetric accretion of non-relativistic gas onto compact objects, this work was also the generalization of Bondi and Hoyle earlier work [4]. It may be noted that the Bondi's work was distinct from Hoyle and Lyttleton's [2] works in the sense that accreting gas was at rest at infinity in the former case, while it has finite velocity in the later case. So far entire work was done using Newtonian gravity. A relativistic generalization was made by Michel [5] (see also [6] for further generalizations and supplements to Michel's solution) who studied the stationary, spherically symmetric and relativistic accretion onto the compact objects. Several generalization to Michel's work have been suggested to discuss accretion in various other form [6, 7], viz., properties of the accretion onto Schwarzschild black hole has been broadly investigated in [8–11] and Begelman [12] examined some aspects of critical points of accretion problem. Other include the accretion onto a higher dimensional black hole [13, 14], onto a black hole in the string cloud background in [15], onto a charged black hole [16–18] and onto a rotating black hole [19, 20] (see all review [21]). A study of general relativistic spherical accretion with and without back-reaction has also been done in [22] and the result showed that the mass accretion rate is enhanced in the absence of back-reaction.

The aim of this work is to explicitly bring out the NC geometrical effects on the spherically symmetric accretion onto Schwarzschild black holes. It is well known that the accretion process is a powerful indicator of the physical nature of the central celestial objects, which means that the analysis of the accretion around the nonrotating NC inspired black hole could help us to understand the regime where general relativity breaks down.

However, even after intensive research on black holes some aspects still require cogent interpretation, such as an inadequate description of the late stage black hole evaporation [23]. Still, we can explain black hole evaporation as a semiclassical process, but the breakdown happens in the limit $M_{BH} < M_{pl}$ during evaporation. And furthermore, the black hole temperature ($T_H \approx 1/M$) diverges in the last stage of the evaporation process, that is $T_H \to \infty$ as $M \to 0$. However, one can expect that this divergence will not occur actually, because in the Planck phase the black hole will be dramatically disturbed by the strong quantum gravitational effects under $M_{BH} < M_{pl}$. To efficiently describe all evaporation phases of black hole one must include the quantum field theory (QFT) effects in curved space-time and ensure the controlled behavior of theory at very high energies [24]. The Noncommutativity (NCY) is one of the promising ways to approach QFT in curved space-time [25–28], which arises naturally in the string theories [29]. Since it had been widely accepted that quantum gravity must have an uncertainty

*Electronic address: rahul.phy3@gmail.com
†Electronic address: sghosh2@jmi.ac.in

principle which prevents the exact position measurement below the Planck scale. The NC geometry is naturally encoded in the commutator

$$[x^\mu, x^\nu] = i\theta^{\mu\nu}, \quad [\partial_\mu, \partial_\nu] = 0, \tag{1}$$

where $\theta^{\mu\nu}$ is an anti-symmetric real matrix which determines a discretization of the spacetime. This commutator leads toward the resulting uncertainty relation in quantum gravity regime.

$$\Delta x^\mu \Delta x^\nu \geq \frac{1}{2}|\theta^{\mu\nu}|. \tag{2}$$

Therefore, NC geometry provides a subtle way to space-time quantization and it remove the short-distance divergences of theory as one of the most promising feature.

It may be noted that study of NC geometry inspired black hole are very important as it cures usual problem encountered in the terminal phase of the classical black hole evaporation. Further, the NC inspired black hole has no curvature singularity rather it has de Sitter core at short distance. Many authors have extended classical black hole solution to find exact NC inspired black holes [30]. In this paper, we study the effect of NC geometry upon spherically symmetric accretion onto NC geometry inspired Schwarzschild black hole. Interestingly, it turns out that the mass accretion rate $\dot{M}$ surprisingly decrease in comparison to the Schwarzschild black hole [5].

The paper is organized as follows In Sec. II, we review the NC inspired black hole and study its properties. In Sec. III, the analytic relativistic accretion onto a NC inspired Schwarzschild black hole model is appropriately developed. We calculate how the presence of a smeared mass object instead of point mass object would affect the mass accretion rate $\dot{M}$ of a gas onto a black hole. We also determine analytic corrections to the critical radius, the critical fluid velocity and to the sound speed. We then obtain expressions for the asymptotic behavior of the fluid density and the temperature near the event horizon in Sec. IV. Finally we conclude in Sec.V.

We use the following values for the physical constants for numerical computations and plots: $c = 3.00 \times 10^{10}\mathsf{cm.s}^{-1}$, $G = 6.674 \times 10^{-8}\mathsf{cm}^3\mathsf{.g}.^{-1}\mathsf{s}^{-2}$, $k_B = 1.380 \times 10^{-16}\mathsf{erg.K}^{-1}$, $M = M_\odot = 1.989 \times 10^{33}\mathsf{g}$, $m_b = m_p = 1.67 \times 10^{-24}\mathsf{g}$, $n_\infty = 1\mathsf{cm}^{-3}$, $T_\infty = 10^4\mathsf{K}$.

II. NONCOMMUTATIVE GEOMETRY INSPIRED BLACK HOLE

The analytic relativistic accretion solution onto the black hole by Michel [5] is generalized by considering a NC inspired Schwarzschild black hole. We begin with a brief review of NC inspired Schwarzschild black hole and its properties (see [30] for further details). In the high energy physics, the interest about NCY become very important when, in the theory of open strings [31], the space-time coordinates become non commuting operators. NC geometry is currently employed to implement the fuzziness of space-time by replacing the position Dirac's delta function by spatially spreading Gaussian distribution [25, 26]. We consider the mass density of gravitational source as Gaussian distribution of minimal width $\sqrt{\theta}$, inspired by NC geometry [30],

$$\rho_\theta(r) = \frac{M}{(4\pi\theta)^{3/2}} \exp(-r^2/4\theta). \tag{3}$$

The particle mass M is diffused throughout a region of linear size $\sqrt{\theta}$ and beyond energy scale $1/\sqrt{\theta}$ space-time becomes NC.
For Schwarzschild-like geometry $g_{tt} = -(g_{rr})^{-1}$ (or $T_0^0 = T_1^1$), we have to consider

$$T_\theta^\theta = -\rho_\theta - \frac{r}{2}\partial_r\rho\theta, \tag{4}$$

under NC geometry a massive point source turns into a self-gravitating, anisotropic fluid-type matter of density ρ_θ and pressure $P_r = -\rho_\theta$, $P_{||} = -\rho_\theta - \frac{r}{2}\partial_r\rho_\theta$. Thus Schwarzschild solution in NC geometry has

$$\phi(r) = -\frac{GM}{r} erf\left(\frac{r}{2\sqrt{\theta}}\right), \tag{5}$$

which matches with the Newtonian potential at large distances, and differ exponentially at short distance, at $r = 0$, here $\phi(r)$ reads as

$$\phi(0) = -\frac{GM}{\sqrt{\pi\theta}}.$$

Hence as expected, NC geometry regularize the divergence at short distance. Solving the Einstein equation $G_{ab} = 8\pi T_{ab}$ with matter source (3), we find the line element

$$\begin{aligned} ds^2 &= \left(1 - \frac{4M}{r\sqrt{\pi}}\gamma(3/2, r^2/4\theta)\right)dt^2 \\ &\quad -\left(1 - \frac{4M}{r\sqrt{\pi}}\gamma(3/2, r^2/4\theta)\right)^{-1} dr^2 \\ &\quad -r^2(d\vartheta^2 + sin^2(\vartheta)d\phi^2), \end{aligned} \tag{6}$$

where $\gamma(3/2, r^2/4\theta)$ is the lower incomplete gamma function,

$$\gamma(3/2, r^2/4\theta) = \int_0^{r^2/4\theta} e^{-t}t^{1/2}dt. \tag{7}$$

The classical Schwarzschild solution can be recovered in the limit $r/\sqrt{\theta} \to \infty$, and again in the limit $r \to \infty$, we get Minkowski solution. The event horizon are zeros of $g^{rr}(r_H) = 0$, i.e.,

$$r_H = \frac{4M}{\sqrt{\pi}}\gamma\left(3/2, r_H^2/4\theta\right) \tag{8}$$

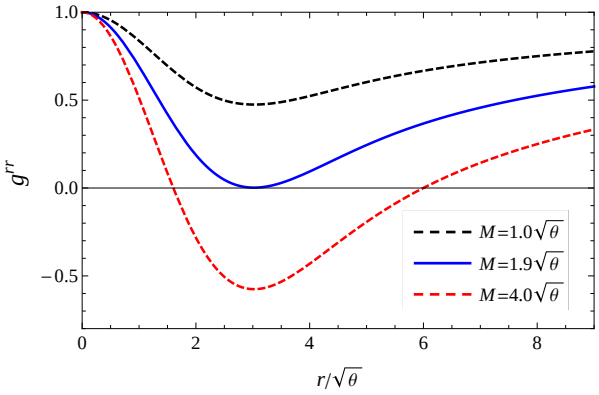

FIG. 1: (Color online) plot $-g_{tt} = g_{rr}^{-1}$ as a function of $r/\sqrt{\theta}$ for various values of $M/\sqrt{\theta}$. $M = 1.0\sqrt{\theta}$ (Black curve) has no horizon, $M = 1.9\sqrt{\theta}$ (Blue curve) has one degenerate horizon at $r_H = 3.0\sqrt{\theta}$, and $M = 4.0\sqrt{\theta}$ (Red curve) has two horizons .

which can be written in terms of upper incomplete gamma function as

$$r_H = 2M\Big(1 - \frac{2}{\sqrt{\pi}}\gamma^u(3/2, M^2/\theta)\Big). \tag{9}$$

The numerical solution for horizon are depicted in Fig. 1, it is clear that NCY modify the behavior of horizon and their radius. It turns out that one can find a critical mass M_0 such that a single degenerate horizon occur for $M = M_0 = 1.9\sqrt{\theta}$ with $r_H = 3\sqrt{\theta}$, for $M > M_0$ there are two horizons, and whereas for $M < M_0$, there is no horizon. The larger root corresponds to the event horizon of the black hole, and the smaller is so called the Cauchy (or inner) horizon. In fact space-time curvature scalars are regular at $r = 0$. One can write, in the large limit, r_H as

$$r_H = 2M\Big(1 - \frac{M}{\sqrt{\theta\pi}}e^{-M^2/\theta}\Big). \tag{10}$$

The effects of NCY fall off exponentially and are only of relevance at the small distance where space-time fuzziness come into the picture. Hence, clearly NC inspired black hole horizon radius r_H is always less than or equal to the conventional black hole horizon radius $2M$, $r_H \leq 2M$.

Also, the mass of the black hole can be obtained by integrating Eq. (3) as

$$m_\theta(r) = \int_0^r 4\pi\, s^2\, \rho(s)\, ds = \frac{2M}{\sqrt{\pi}}\gamma(3/2, r^2/4\theta) = Mf(r) \tag{11}$$

and hence the line element can be conveniently put in the form

$$\begin{aligned} ds^2 &= \Big(1 - \frac{2Mf(r)}{r}\Big)dt^2 - \frac{1}{\Big(1 - \frac{2Mf(r)}{r}\Big)}dr^2 \\ &\quad -r^2(d\vartheta^2 + sin^2(\vartheta)d\phi^2). \end{aligned} \tag{12}$$

where

$$f(r) = \frac{2}{\sqrt{\pi}}\gamma(3/2, r^2/4\theta), \tag{13}$$

in the limit, $r/\sqrt{\theta} \to \infty$, $f(r) = 1$. The metric (12) is useful to discuss the properties of accretion onto NC inspired black hole which is analyzed in the next section.

III. ACCRETION ONTO BLACK HOLE

Here, we generalize the results of the relativistic accretion onto the NC inspired Schwarzschild black hole and analyze how the NCY demand a transition to supersonic flow in the solution. A black hole will capture the interstellar ambient matter presents within a certain effective distance. Due to spherical symmetry this accretion will be a steady-state radial inflow of gas [5, 7]. The gas is approximated as isotropic, though inhomogeneous perfect fluid, inhomogeneity in fluid is due to the fact that near accreting body energy density of gas will be position dependent, and described by the stress-energy tensor

$$T^{\mu\nu} = (\rho + p)\, u^\mu u^\nu + p g^{\mu\nu}, \tag{14}$$

where ρ and p are the fluid energy density and pressure in the comoving frame, respectively, and

$$u^\mu = \frac{dx^\mu}{d\tau}, \tag{15}$$

is the fluid's proper four-velocity define with respect to the proper time τ. In the comoving frame, baryon number density n, and the baryon number flux are related as $J^\mu = nu^\mu$. The conservation of baryon number flux

$$\nabla_\mu J^\mu = \nabla_\mu(nu^\mu) = 0, \tag{16}$$

and conservation of stress-energy tensor yields,

$$\nabla_\mu T^\mu_\nu = 0. \tag{17}$$

With the normalization condition $u_\mu u^\mu = -1$, and due to the restriction of spherically symmetric accretion, the velocity components become $u^\vartheta = 0, u^\phi = 0$; $u^\mu = (u^0, u^1(= v(r)), 0, 0)$, we have

$$u^0 = \left[\frac{v^2 + 1 - \frac{2Mf(r)}{r}}{\Big(1 - \frac{2Mf(r)}{r}\Big)^2}\right]^{1/2}. \tag{18}$$

We rewrite Eq. (16) as

$$\frac{1}{r^2}\frac{d}{dr}\left(r^2 nv\right) = 0, \tag{19}$$

We now calculate the three-velocity of the accreting fluid for distant observer, defined by $w = u^i u_i$,

$$\begin{aligned} w &= \frac{u^1}{u^0}\left(\frac{1}{1 - \frac{2Mf(r)}{r}}\right), \\ &= \frac{v}{(1 - \frac{2Mf(r)}{r} + v^2)^{1/2}}. \end{aligned} \tag{20}$$

The assumption of spherical symmetry and steady state radial inflow reformulate Eq. (17) in a simple form. The $\nu = 0$ component yield as

$$\frac{1}{r^2}\frac{d}{dr}\left[r^2(\rho+p)v\left(1-\frac{2Mf(r)}{r}+v^2\right)^{1/2}\right]=0. \quad (21)$$

and $\nu = 1$ component can be simplified to

$$v\frac{dv}{dr}=-\left(\frac{1-\frac{2Mf(r)}{r}+v^2}{\rho+p}\right)\frac{dp}{dr}-\frac{Mf(r)}{r^2}+\frac{M}{r^2}\frac{df(r)}{dr}. \quad (22)$$

The above equations are generalization of result obtained for standard black hole.

A. Accretion process

We are considering spherical steady state accretion onto a NC inspired Schwarzschild black hole of mass M, and the boundary conditions at infinity are same as the Schwarzschild black hole [5]. Since there is no entropy production for adiabatic fluid, hence the mass conservation equation reads

$$Tds = 0 = d\left(\frac{\rho}{n}\right)+p\,d\left(\frac{1}{n}\right), \quad (23)$$

which may be rewritten as

$$\frac{d\rho}{dn}=\frac{\rho+p}{n}. \quad (24)$$

A crucial physical entity in accretion process is speed of sound a defined as [7],

$$a^2\equiv\frac{dp}{d\rho}=\frac{dp}{dn}\frac{n}{\rho+p}. \quad (25)$$

The baryon conservation given by Eq. (16) and the momentum conservation reads

$$(\rho+p)u^{\mu}_{;\mu}+u^{\mu}\rho_{,\mu}=0, \quad (26)$$

on inserting Eq. (25) in Eqs. (16) and (26), these modifies to

$$\frac{v'}{v}+\frac{n'}{n}+\frac{2}{r}=0, \quad (27)$$

$$\left[vv'+a^2\left(1-\frac{2Mf(r)}{r}+v^2\right)\frac{n'}{n}+\frac{Mf(r)}{r^2}-\frac{M}{r}\frac{df(r)}{dr}\right]=0, \quad (28)$$

where a dash ($'$) denotes a spatial derivative. Solving the coupled Eqs. (27) and (28) simultaneously

$$v'=\frac{N_1}{N}, \quad (29a)$$

$$n'=-\frac{N_2}{N}. \quad (29b)$$

These are known as Bondi equation [3], with

$$N_1=\frac{1}{nr^2}\left[\left(1-\frac{2Mf(r)}{r}+v^2\right)2a^2r-Mf(r)+Mrf'(r)\right], \quad (30a)$$

$$N_2=\frac{1}{vr^2}\left[2v^2r-Mf(r)+Mrf'(r)\right], \quad (30b)$$

$$N=\frac{1}{vn}\left[v^2-\left(1-\frac{2Mf(r)}{r}+v^2\right)a^2\right]. \quad (30c)$$

For same boundary conditions there are various classes of solution but we are only interested in which velocity increases monotonically from $v = 0$ at $r = \infty$ to $v = 1$ at $r = r_H$. For large r, the flow is subsonic i.e. $v < a$ and since the sound speed must be sub-luminal, i.e., $a^2 < 1$, this assure $v^2 \ll 1$. Therefore, the denominator of Eq. (29) define by Eq. (30c), takes the form

$$N\approx\frac{v^2-a^2}{vn}<0, \quad (31)$$

at the event horizon $r_H = 2Mf(r_H)$, again under the causality constraint, $a^2 < 1$, hence

$$N=\frac{v(1-a^2)}{n}>0. \quad (32)$$

Therefore from Eqs. (31) and (32), the flow must pass through a critical point $r_H < r_s < \infty$, where $N = 0$. The steady and continuous radial inflow demands $N_1 = N_2 = 0$ at r_s, otherwise turn-around point will occur in trajectory and solution will be double valued in either r or v. This is nothing but the so-called *sonic condition* and r_s is called sonic radius. The solution of Eq. (29) crossing the critical point known as transonic solution. At $r = r_s$ from the Eq. (30), we find that

$$v_s^2=\frac{a_s^2}{1-a_s^2}\left[1-\frac{2Mf(r_s)}{r_s}\right]=\frac{M}{2r_s}\left[f(r_s)-r_sf'(r_s)\right], \quad (33)$$

where $v_s \equiv v(r_s)$ and $a_s \equiv a(r_s)$. The quantities with a subscript s are defined at sonic points of the flow. It is clear from Eqs. (20) and (33), that at critical point r_s, accreting fluid speed will be $w_s = a_s$. For the standard Schwarzschild black hole $f(r) = 1$, we get the celebrated result of Michel's work, reads as

$${v_s}^2=\frac{M}{2r_s}=\frac{a_s^2}{1+3a_s^2}. \quad (34)$$

It can be clearly seen that the critical velocity in this model is modified by NC geometry parameter, and the physically acceptable solution $v_s^2 > 0$ is guaranteed from Eq. (33).

Bondi mass accretion rate can be obtain by integrating Eq. (19) over a 4-dimensional volume and multiply by m_b, the mass of each baryon, to get

$$\dot{M}=4\pi r^2m_bnv, \quad (35)$$

where $\dot{M}$ is mass accretion rate having dimension of mass per unit time. The most influencing equations for study accretion are Eqs. (19) and (21), and collectively these yield to

$$\left(\frac{\rho+p}{n}\right)^2\left(1-\frac{2Mf(r)}{r}+v^2\right)=\left(\frac{\rho_\infty+p_\infty}{n_\infty}\right)^2, \quad (36)$$

which is the improved relativistic Bernoulli equation for the steady state accretion onto NC inspired black holes where the back-reaction of fluid is ignored. Equations (35) and (36) are the characteristic equation of accretion with parameter θ. In the limit $r/\sqrt{\theta}\to\infty$, our results reduce to the standard Schwarzschild black hole obtained in [5, 7].

B. The polytropic solution

We are considering the case when the critical point lie outside the outer horizon of improved Schwarzschild black hole. To calculate $\dot{M}$ following Bondi [3] and Michel [5], we introduce a polytropic equation of state for a fluid,

$$p=Kn^\Gamma, \quad (37)$$

where K and the adiabatic index Γ are constants. Using Eq. (37) in (23), and integration leads to

$$\rho=\frac{K}{\Gamma-1}n^\Gamma+m_b n, \quad (38)$$

where m_b is an integration constant, and is evaluated on comparing with $\rho=m_b n+\epsilon$ with ϵ as internal density. Hence Eqs. (37) and (38) with Eq. (25) give

$$\Gamma K n^{\Gamma-1}=\frac{a^2 m_b}{(1-\frac{a^2}{\Gamma-1})}. \quad (39)$$

Further, substituting Eqs. (38) and (39), in the Bernoulli equation (36), we obtain

$$\left(1+\frac{a^2}{\Gamma-1-a^2}\right)^2\left(1-\frac{2Mf(r)}{r}+v^2\right)=\left(1+\frac{a_\infty^2}{\Gamma-1-a_\infty^2}\right)^2. \quad (40)$$

This equation will also be true at critical radius r_s, using the relation (33), we get

$$\left(1-\frac{a_s^2}{\Gamma-1}\right)^2\left(1-\frac{2Mf(r_s)}{r_s}\right)^{-1}(1-a_s^2)=\left(1-\frac{a_\infty^2}{\Gamma-1}\right)^2. \quad (41)$$

For large but finite values of r, i.e. $r\geq r_s$, it is likely that baryons will be non-relativistic. In this regime, we should have $a\leq a_s\ll 1$. Expanding Eq. (41) up to second order in a_s and a_∞, we find

$$\left(\frac{\Gamma+1}{\Gamma-1}\right)a_s^2=\frac{2a_\infty^2}{\Gamma-1}+\frac{2Mf(r_s)}{r_s}\left[\frac{(\Gamma-1)-2a_\infty^2}{\Gamma-1}\right]. \quad (42)$$

Clearly, for $a_s^2>0$, we have

$$r_s>2Mf(r_s)\Rightarrow r_s>r_H\left[\frac{f(r_s)}{f(r_H)}\right]. \quad (43)$$

In the limit $r/\sqrt{\theta}\to\infty$, from Eqs. (34) and (40), we obtain

$$a_s^2=\frac{2}{5-3\Gamma}a_\infty^2. \quad (44)$$

We note from Eqs. (42) and (44) that sound speed at critical point enhanced due to NC effect. From Eqs. (33) and (42):

$$r_s=\frac{(5-3\Gamma)Mf(r_s)\left[2a_\infty^2-(\Gamma-1)\right]}{4a_\infty^2(1-\Gamma)+Mf'(r_s)(\Gamma+1)\left[2a_\infty^2-(\Gamma-1)\right]}, \quad (45)$$

this is the critical radius for polytropic fluid of adiabatic index Γ. For $a_\infty^2/(\Gamma-1)\ll 1$, we get

$$r_s\approx\frac{(5-3\Gamma)f(r_s)}{(\Gamma+1)f'(r_s)}, \quad (46)$$

and under commutative consideration $r/\sqrt{\theta}\to\infty$, we get the standard result for Schwarzschild black hole accretion, reads

$$r_s=\frac{(5-3\Gamma)}{4}\frac{M}{a_\infty^2}. \quad (47)$$

It may be noted from Eqs. (45) and (47) that critical radius decrease in the case of NC inspired black hole, and this will put influential impact upon mass accretion rate and other characteristics of the accretion. Under the limiting case $a^2/(\Gamma-1)\ll 1$, Eq. (39) will take the form

$$\frac{n}{n_\infty}\approx\left(\frac{a}{a_\infty}\right)^{2/(\Gamma-1)}. \quad (48)$$

Accretion rate $\dot{M}$ (35) must also hold for $r=r_s$. At critical point Bondi accretion rate is given as

$$\dot{M}=4\pi r_s^2 m_b n_s v_s. \quad (49)$$

By virtue of Eqs. (33), (42), (45) and (48) the accretion rate becomes

$$\dot{M}=2\pi\left(\frac{a_s}{a_\infty}\right)^{2/(\Gamma-1)} r_s\left(f[r_s]-r_s f'[r_s]\right)(m_b n_\infty M). \quad (50)$$

The accretion rate has mass dependency as $\dot{M}\sim M^2$, which is similar to that of the Newtonian model [3] as well

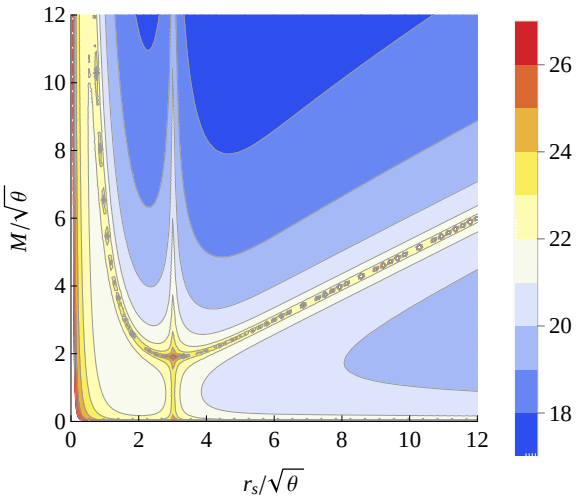

FIG. 2: Mass accretion rate for accreting gase of $\Gamma = 1.5$ is plotted along the color axes as a function of $r_s/\sqrt{\theta}$ and $M/\sqrt{\theta}$.

as the relativistic case [5, 7]. If no effects of NC geometry are taken into account, then substituting Eqs. (34), (44) and (47), into Eq. (49), we get the well known result derived in [5, 7],

$$\dot{M} = 4\pi\lambda_s(m_b n_\infty M^2 a_\infty^{-3}), \tag{51}$$

with

$$\lambda_s = \left(\frac{1}{2}\right)^{(\Gamma+1)/2(\Gamma-1)} \left(\frac{5-3\Gamma}{4}\right)^{-(5-3\Gamma)/2(\Gamma-1)}. \tag{52}$$

In Fig. 2, we have plotted the logarithm of the accretion rate $\dot{M}$ against the $r_s/\sqrt{\theta}$ and $M/\sqrt{\theta}$.

C. Some Numerical Results

The most essential equations characterizing accretion of fluid are Eqs. (19) and (40). Even though they look simple, still these equations are difficult to solve analytically. To get a numerical solution [17], it is a feasible idea to work with dimensionless variables i.e., the radial distance ($x = r/2M$) and the particle number density ($y = n/n_\infty$). In terms of these newly defined variables Eq. (40) can be reexpressed as,

$$\left(1 + \frac{a_\infty^2}{\Gamma-1} y^{\Gamma-1}\right)^2 \left(1 - \frac{f(2Mx)}{x} + v^2\right) = \left(1 + \frac{a_\infty^2}{\Gamma-1}\right)^2. \tag{53}$$

While the baryon conservation equation (19) will take the form

$$nvr^2 = n_s v_s r_s^2,$$

it can be recast as

$$yv = \left(\frac{x_s}{x}\right)^2 \left(\frac{n_s}{n_\infty}\right) v_s. \tag{54}$$

Following Eq. (48), we get

$$yv = \left(\frac{x_s}{x}\right)^2 \left(\frac{a_s}{a_\infty}\right)^{2/(\Gamma-1)} v_s. \tag{55}$$

Now we are left with two non-linear equations (53) and (55), which can be easily solved numerically for both the fluid velocity v and the compression ratio y. The velocity profile for the radial inflow of accreting fluid $\Gamma = 1.5$ as a function of the dimensionless variable x is plotted in Fig. 3.

The event horizon r_H for the NC inspired black hole, has profound dependency upon θ. From Fig. 3, it is evident that accreting fluid cross event horizon with speed of light. For example, a black hole of mass $M = 1.92\sqrt{\theta}$ has outer horizon radius $r_H = 3.276\sqrt{\theta} < 2M$, mass $M = 1.94\sqrt{\theta}$ has $r_H = 3.4115\sqrt{\theta}$, mass $M = 1.96\sqrt{\theta}$ has $r_H = 3.5154\sqrt{\theta}$, mass $M = 2.0\sqrt{\theta}$ has $r_H = 3.68\sqrt{\theta}$ and for $M = 40\sqrt{\theta}$ horizon radius is $r_H \approx 80\sqrt{\theta}(= 2M)$. Clearly, NC effects are subjugate for low mass regime. In Fig. 4, we compare the radial velocity profile of accreting gas for NC inspired black hole with the conventional black hole.

The variation of compression ratio y as a function of radial coordinate for a accreting gas with $\Gamma = 1.5$ is shown in Fig. 5. Since we have shown that black hole mass is a dynamical quantity governed by modified Bondi accretion rate. Total integrated flux due to surface luminosity L_ν reads

$$F_\nu = \frac{L_\nu}{4\pi d_L^2}, \tag{56}$$

where surface luminosity is proportional to accretion rate $L_\nu \propto \dot{M}$. This integrated flux modify due to NC behavior of black hole, therefore extra integrated flux as compare to conventional black hole is

$$F = \frac{F_\nu - F_{\nu 0}}{F_{\nu 0}}, \tag{57}$$

where F_ν and $F_{\nu 0}$ are flux for NC inspired black hole and for conventional black hole, respectively. For $M >> M_0$, we have $F_{\nu 0} >> F_\nu$, therefore $F \sim -1$. This is due to the fact that accretion radius decreases due to NC effects and so accretion rate too.

IV. ASYMPTOTIC BEHAVIOUR

In the previous section, we mainly discuss the characteristic of accretion for the case where critical point is far away from outer horizon i.e., $r_s \gg r_H$. In this section, we will explore the other possibilities $r_H < r \ll r_s$ and

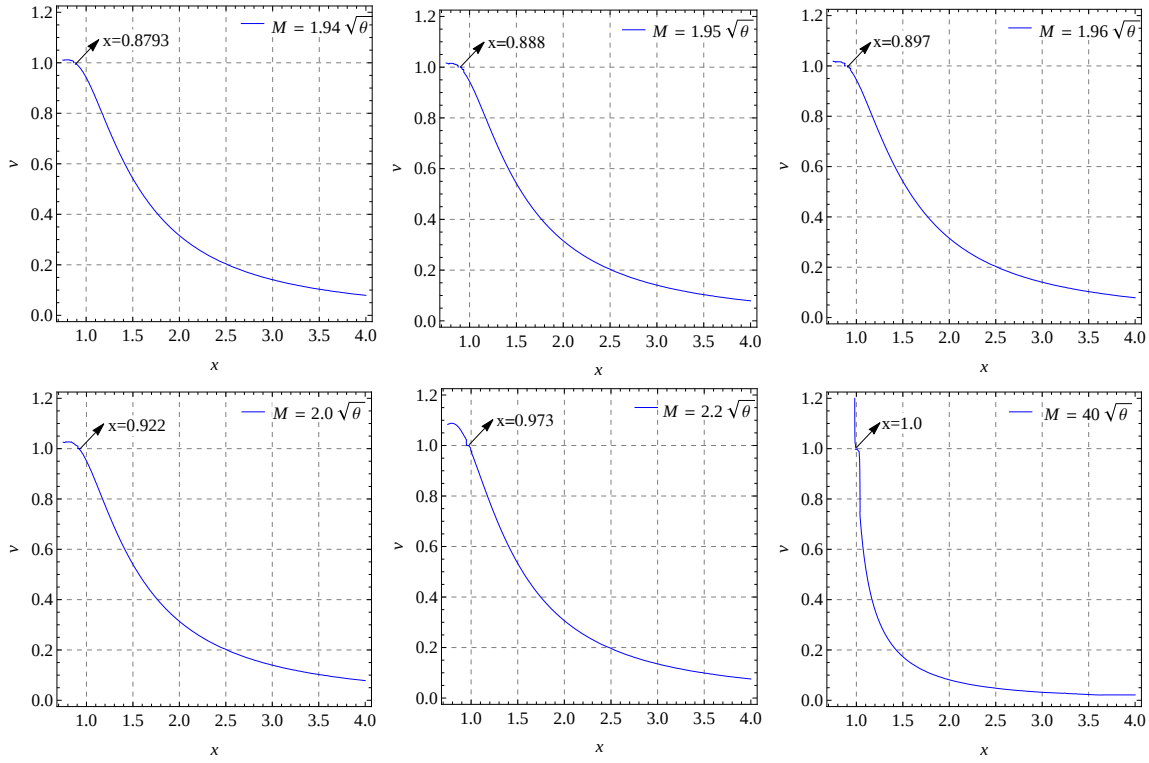

FIG. 3: Plot showing the radial velocity profile v for fluid $\Gamma = 1.5$ accreting onto the noncommutative inspired black hole as a function of dimensionless radius x.

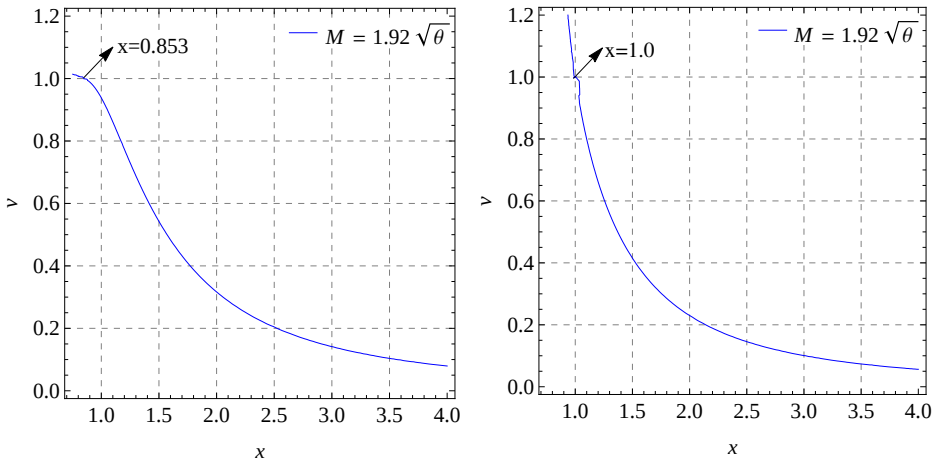

FIG. 4: The radial velocity profile v for fluid $\Gamma = 1.5$ accreting onto the black hole as a function of dimensionless radius x. (Left) NC inspired black hole. (Right) Conventional black hole.

at the event horizon $r = r_H$.

The radial inflow solution is transonic in nature, therefore for case $r < r_s$, fluid will be supersonic $v > a$. Near the horizon we can safely consider that

$$v^2 \approx \frac{2Mf(r)}{r}, \qquad \Gamma \neq \frac{5}{3}. \tag{58}$$

Similarly the gas compression ratio will also get altered by using Eqs. (19) and (48) as

$$\frac{n(r)}{n_\infty} \approx \left(\frac{n_s}{n_\infty}\right) \frac{r_s^2 v_s}{\sqrt{2Mf(r)r^3}}, \tag{59}$$

$$\frac{n_s}{n_\infty} = \left[\frac{1}{(\Gamma+1)} 2r_s - \frac{2Mf(r_s)}{a_\infty^2}(2a_\infty^2 + (\Gamma - 1))\right]^{1/(\Gamma-1)} \tag{60}$$

For large r values, $f(r) \approx 1$, and therefore accretion situation will not much differ from the standard commuta-

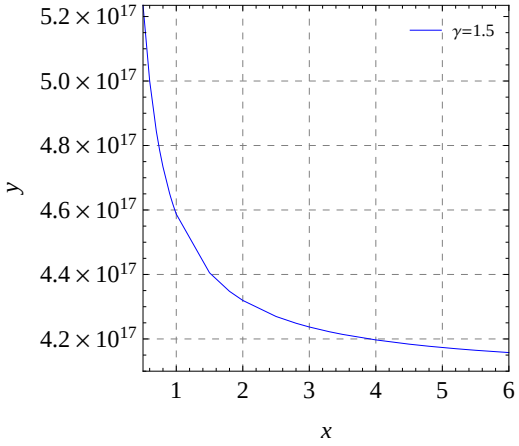

FIG. 5: The compression factor (y) for fluid $\Gamma = 1.5$ accreting onto the black hole with $M = 40\sqrt{\theta}$ as a function of dimensionless radius x.

tive accretion. However, at the small distance, $f(r) \ll 1$ and hence, number density at distance r will get modify comparing to standard spherical accretion. Assuming a gas follow the fundamental thermodynamic, $p = nk_BT$, we find the adiabatic temperature profile using Eqs. (37) and (59):

$$\frac{T(r)}{T_\infty} = \left[\frac{n(r)}{n_\infty}\right]^{\Gamma-1}. \tag{61}$$

Next, at the event horizon of NC inspired black hole, we have $r_H = 2Mf(r_H)$ and at a distance less than Bondi radius gas is always supersonic. Near horizon gas is always relativistic and rationally we can take, $v_H^2 \equiv v^2(r_H) \approx 1$. Consequently, gas compression ratio gets modify as:

$$\frac{n_H}{n_\infty} \approx \left(\frac{n_s}{n_\infty}\right)\frac{r_s^2 v_s}{{r_H}^2}. \tag{62}$$

The effect of NC geometry at black hole horizon can be noticed from the fact that for low mass black hole, horizon radius decrease due to NC effects, which will significantly change the number density at the horizon.

V. CONCLUSIONS

Recent years witnessed a flurry of activities toward research devoted to NC inspired black hole physics, and one can assert that it is induced by the string theory. The NC geometry provides an effective framework to study short-distance space-time dynamics. It turns out that NC inspired Schwarzschild black hole smoothly interpolate between a de Sitter core around the origin and ordinary Schwarzschild black hole at large distance. It has exquisite effects on black holes, such as it turn ordinary Schwarzschild black hole into the regular black hole with two horizons, furthermore the compelling modification in late stage evaporation of black hole. Further, the accretion of the matter onto black hole is one of the acceptable idea to explain the ultra high energy output from the active galactic nuclei and the quasars.

This paper deals with basic model of steady state spherical accretion of a polytropic fluid onto NC inspired Schwarzschild black hole. Resultant radial inflow of fluid is transonic in character even for conventional black hole [3]. But other accretion parameters such as critical radius r_s, sonic speed a_s, accretion rate $\dot{M}$ and other thermodynamic quantities such as gas compression ratio y, the temperature at various distance from the horizon $T(r)$ get modify substantially due to NCY. Even though critical point locates away from the outer horizon of black hole, but it has subtle dependency over NC parameter θ. Due to NC effects critical radius seems to decrease as compare to conventional black hole, but on the other hand sound speed at critical point increases. Thus, despite of the NCY complexity, we have determined analytically the critical radius, critical fluid velocity and sound speed, and subsequently the mass accretion rate. We then obtain expressions for the asymptopic behaviour of the fluid density and temperature near the event horizon. Hence, in this sense, we may conclude that the steady state spherical accretion solution onto the Schwarzschild black hole is stable. In the limit $r/\sqrt{\theta} \to \infty$, the results obtained here reduced exactly to vis-à-vis to those obtained by [5].

Acknowledgements

S.G.G. would like to thanks SERB-DST Research Project Grant No. SB/S2/HEP-008/2014 and DST INDO-SA bilateral project DST/INT/South Africa/P-06/2016 and also to IUCAA, Pune for the hospitality while this work was being done. R.K. would like to thanks UGC for providing Junior Research Fellowship.

Note Added in Proof: After this work was completed, we learned of a similar work by Biplab et al. [32], which appeared on 30th March 2017 in arXiv .

[1] Ignacio Gonzlez Martnez-Pas, Tariq Shahbaz, Jorge Casares Velzquez, Accretion Processes in Astrophysics, Cambridge University Press, 2014.
[2] F. Hoyle, R. A. Lyttelton, Proc. Cambridge Philos. Soc. **35**, 405 (1939).
[3] H. Bondi, Mon. Not. Roy. Astron. Soc. **112**, 195 (1952).
[4] H. Bondi, F. Hoyle, Mon. Not. Roy. Astron. Soc. **104**, 273 (1944).
[5] F.C. Michel, Astrophys. Space Sci. **15**, 153 (1972).
[6] B. J. Carr and S.W. Hawking, Mon. Not. R. Astron. Soc.

168, 399 (1974); D. Ray, Astron. Astrophys. **82**, 368 (1980); K.S. Thorne, R.A. Flammang and A.N. Zytkow, Mon. Not. R. Astron. Soc. **194**, 475 (1981); E. Bettwieser and W. Glatzel, Astron. Astrophys. **94**, 306 (1981); K.M. Chang, Astron. Astrophys. **142**, 212 (1985); U.S. Pandey, Astrophys. Space Sci. **136**, 195 (1987).

[7] S.L. Shapiro and S.A. Teukolsky, *Black Holes, White Dwarfs and Neutron Stars: The Physics of Compact Objects* (Wiley, New York, 1983).

[8] E. Babichev, V. Dokuchaev and Y. Eroshenko, Phys. Rev. Lett. **93**, 021102 (2004);

[9] E. Babichev, V. Dokuchaev and Y. Eroshenko, Zh. Eksp. Teor. Fiz. **127**, 597 (2004).

[10] E. Babichev, V. Dokuchaev and Y. Eroshenko, J. Exp. Theor. Phys. **100**, 528 (2005);

[11] E. Babichev, V. Dokuchaev and Y. Eroshenko, AIP Conf. Proc. **861**, 554 (2006).

[12] M.C. Begelman, Astron. Astrophys. **70**, 583 (1978).

[13] M. Sharif and G. Abbas, Mod. Phys. Lett. A **26**, 1731 (2011).

[14] A.J. John, S.G. Ghosh and S.D. Maharaj, Phys. Rev. D **88**, 104005 (2013).

[15] A. Ganguly, S. G. Ghosh, S. D. Maharaj, Phys. Rev. D **90**, 064037 (2014).

[16] M. Jamil, M.A. Rashid and A. Qadir, Eur. Phys. J. C **58**, 325 (2008).

[17] J. A. de Freitas Pacheco, Journal of Thermodynamics **2012**, 791870 (2012).

[18] E. Babichev, S. Chernov, V. Dokuchaev and Y. Eroshenko, J. Exp. Theor. Phys. **112**, 784 (2011).

[19] S.L. Shapiro, Astrophys. J. **185**, 69 (1973).

[20] S.L. Shapiro, Astrophys. J. **189**, 343 (1974).

[21] B. J. Carr, T. Harada and H. Maeda, Class. Quant. Grav. **27**, 183101 (2010)

[22] E. Malec, Phys. Rev. D **60**, 104043 (1999).

[23] S. W. Hawking, Comm. Math. Phys. **43**, 199 (1975).

[24] T. Padmanabhan, Phys. Rep. **406**, 49 (2005).

[25] A. Smailagic, E. Spallucci, J. Phys. **A43**, L467 (2003).

[26] A. Smailagic, E. Spallucci, J. Phys. **A43**, L517 (2003).

[27] M. Chaichian, A. Demichev, P. Presnajder, Nucl. Phys. **B567**, 360 (2000); S. Cho, R. Hinterding, J. Madore, H. Steinacker,Int. J. Mod. Phys. **D9**, 161 (2000).

[28] A. Smailagic, E. Spallucci, J. Phys. **A37**, 7169 (2004).

[29] A. Connes, M.R. Douglas, A. Schwarz, JHEP 9802 (1998) 003; N. Seiberg, E. Witten, JHEP 9909 (1999) 032, hep-th/9908142.

[30] P. Nicolini, A. Smailagic and E. Spallucci, Phys. Lett. B **632**, 547 (2006).

[31] E. Witten,Nucl. Phys. B 268, 253 (1986); N. Seiberg and E. Witten, JHEP 09, 032 (1999)

[32] B. Paik and S. Gangopadhyay, arXiv:1703.10057.